

SEMI-PARAMETRIC LEAST-AREA LINEAR-CIRCULAR REGRESSION THROUGH MOBIUS TRANSFORMATION

Surojit Biswas
surojit23@iitkgp.ac.in
and
Buddhananda Banerjee
bbanerjee@maths.iitkgp.ac.in

Department of Mathematics
IIT Kharagpur, India-721302

ABSTRACT. This paper introduces a new area-based regression model where the responses are angular variables and the predictors are linear. The regression curve is formulated using a generalized Möbius transformation that maps the real axis to the circle. A novel area-based loss function is introduced for parameter estimation, utilizing the intrinsic geometry of a curved torus. The model is semi-parametric, requiring no specific distributional assumptions for the angular error. Extensive simulation studies are performed with von Mises and wrapped Cauchy distributions as angular errors. The practical utility of the model is illustrated through real data analysis of two well-known cryptocurrencies, Bitcoin and Ethereum.

⁰corresponding author: bbanerjee@maths.iitkgp.ac.in

1. INTRODUCTION

In statistics, directional data is an area that addresses measurements confined to angular spaces, making it distinctly different from standard linear data due to its periodic nature. This type of data is commonly encountered in fields such as meteorology, where wind directions are recorded, biology, where animal movement patterns are studied, and finance, where the timing of the highest or lowest price is analyzed. A particularly interesting extension of directional data analysis involves cylindrical data structures. Cylindrical data incorporates both an angular (circular) component and a linear (height or distance) component, creating a framework suited to analyzing variables that vary in both direction and magnitude. For example, in finance, the time of occurrence of the highest or lowest price is represented as angular variable, while the price itself is treated as a linear variable. Similarly, in environmental science, wind measurements often include both direction (angular) and speed (linear), effectively forming cylindrical data. Linear-circular (Cylindrical) regression is a statistical approach for analyzing the relationship between a circular (angular) variable and a linear variable. In this framework, the response variable is angular, often representing directions, while the predictor variable is linear. The periodic nature of the circular data, typically constrained within a 360° or $[0, 2\pi]$ range, introduces unique challenges compared to traditional linear regression, as standard regression techniques do not account for the cyclical behavior of the data. A common approach is to model the circular outcome as a function of the linear predictor, often by expressing the angular component in terms of sine and cosine functions or tangent functions (see, [Fisher and Lee, 1992](#)) to handle periodicity. By effectively linking circular and linear components, linear-circular regression offers valuable insights into relationships that conventional linear regression methods would otherwise obscure.

A Möbius transformation, also known as a linear fractional transformation, is a function that maps the extended complex plane (including infinity) onto itself in a way that preserves the general structure of lines and circles. It is defined by the function:

$$f(z) = \frac{az + b}{cz + d}$$

where z is a complex variable, and $a, b, c,$ and d are complex constants satisfying $ad - bc \neq 0$ (to ensure the transformation is non-degenerate). This transformation can be decomposed into a sequence of four fundamental types of maps:

- Translation: $f(z) = z + b$, where b is a complex constant.
- Dilation (and scaling): $f(z) = \alpha z$, where α is a real, positive constant.
- Rotation: $f(z) = e^{i\theta}z$, where θ is the rotation angle in radians.
- Inversion (and reflection): $f(z) = \frac{1}{z}$.

Möbius transformations possess several remarkable properties. They are conformal, meaning they preserve angles at every point. They map circles and lines in the complex plane to other circles or lines, making them essential tools in complex analysis. In a seminal paper, [McCullagh \(1996\)](#) explored the use of Möbius transformations in directional statistics to investigate the connection between the real Cauchy distribution and the wrapped Cauchy distribution.

Recently, [Jha and Biswas \(2018\)](#) utilized Möbius transformation as a link function for circular-circular regression, especially on zero-spike data commonly encountered in ophthalmology research. Earlier applications of Möbius transformations in circular-circular regression models can be found in the works of [Downs and Mardia \(2002\)](#), [Downs \(2003\)](#), and [Kato et al. \(2008\)](#). These developments have greatly expanded the scope and utility of Möbius transformations in regression analysis.

Here, a new area-based measurement between two angles $\phi, \theta \in \mathbb{S}_1$ is briefly discussed. The rest of our work will be based on the curved torus defined by the parametric equation

$$X(\phi, \theta) = \{(R + r \cos \theta) \cos \phi, (R + r \cos \theta) \sin \phi, r \sin \theta\} \subset \mathbb{R}^3, \quad (1.1)$$

where R, r are the radii of vertical and horizontal angles associated with the angles ϕ, θ . The parameter space for the curved torus is $\mathbb{S}_1 \times \mathbb{S}_1 = \{(\phi, \theta) : 0 < \phi, \theta < 2\pi\}$, known as flat torus. Using the tools from Riemannian geometry we can calculate (see [Biswas et al., 2024](#)) the area element of the curved torus given by

$$dA = r(R + r \cos \theta) d\phi d\theta \quad (1.2)$$

Now using this area-element [Biswas et al. \(2024\)](#) has introduced a new concept they called it “square of an angle” which is the minimum area between $(0, 0)$ to (θ, θ) on the curved torus and they have denoted it given by $A_C^{(0)}(\theta)$. We will use this new area-based measurement for our regression.

MOTIVATING DATA EXAMPLE Cryptocurrency is an innovative form of digital asset that operates as a decentralised medium of exchange over computer networks, without the need for any central authority like governments or banks. Cryptocurrencies utilize cryptographic techniques to ensure the security of transactions, regulate the generation of new units, and authenticate the transfer of assets by using blockchain technology. The decentralized nature of cryptocurrencies facilitates peer-to-peer transactions and fosters financial inclusion by granting unbanked populations access to financial services. Notable instances include Bitcoin, the groundbreaking digital money, and Ethereum, which introduced smart contracts that allow for programmable and automated transactions. The volatility of cryptocurrency markets and speculative character pose distinct difficulties and opportunities for financial modeling, risk assessment, and regulation altogether.

Extreme cryptocurrency prices whether highs or lows reflect shifts in supply-demand dynamics. Highs and lows throughout the day offer critical insights into market sentiment: a high price signals strong buying interest, whereas a low suggests selling pressure. Open and close prices are especially significant, as they represent the sentiment of the market at the beginning and end of the trading day. Open prices set the initial tone for traders, while close prices can drive after-market decisions and predict the next day’s momentum. Market sentiment also plays a crucial role, with negative news leading to declines and positive endorsements or news triggering price surges. After significant price spikes, investors may sell to secure profits, often causing temporary price decreases. Extreme price events create arbitrage opportunities, allowing traders to profit from price discrepancies across exchanges. The timing of these highs and lows also influences trader psychology; early-day lows may prompt caution, while late-day lows encourage position reassessment. Conversely, early-day highs can foster optimism, while late-day highs may lead to profit-taking. Recognizing when these price extremes occur can help traders identify crucial support and resistance levels, enhancing strategy. Liquidity also impacts price stability; low liquidity periods can heighten price volatility, while high liquidity provides stability. By understanding the timing and significance of high, low, open, and close prices, traders can refine their strategies.

Challenges with this data: Cryptocurrency markets operate continuously, 24 hours a day, 365 days a year, due to their decentralized architecture that enables trading across multiple global exchanges without fixed opening and closing times. Unlike traditional financial markets, which pause for holidays and specific hours, the cryptocurrency market allows traders

to respond instantly to market events regardless of time zone or physical location. This round-the-clock environment introduces heightened volatility, as prices can shift rapidly with the unceasing flow of market data and trading activity. Consequently, sophisticated risk management, real-time data analytics, and algorithmic trading techniques are necessary to capitalize on the continuous fluctuations in market conditions.

Applying linear-circular regression to this context is especially valuable, as it allows us to model the timestamp of extreme cryptocurrency values (a circular variable) as a function of linear predictors, such as opening, closing, high, and low prices. linear-circular regression is well-suited for analyzing timestamps of extreme events within a continuous trading day, as timestamps form a circular variable that repeats over the 24-hour cycle, while price levels act as linear predictors. This approach uncovers potential relationships between market prices and the timing of extreme values, providing insight into how price fluctuations throughout the day affect the likelihood of highs or lows at specific times.

This modeling technique offers significant advantages. It improves predictive accuracy by integrating the impact of prices on the timing of extreme events and assists in managing risk by highlighting periods of increased volatility based on price conditions. Furthermore, it reveals trader sentiment and helps align trading strategies with evolving market dynamics. The continuous availability of data introduces a cyclical pattern in the timestamps, making linear-circular regression a robust alternative to conventional linear methods that fail to address this cyclicity. In sum, linear-circular regression is a powerful tool for traders and analysts aiming to optimize strategies in a perpetually active market environment, allowing for enhanced decision-making based on the interplay of price and time.

This paper presents a novel area-based regression model that connects angular responses with linear predictors using a generalized Möbius transformation, which distinctively maps the real axis onto the circle. The model introduces an innovative area-based loss function that utilizes the intrinsic geometry of a curved torus for parameter estimation. Unlike conventional methods, this semi-parametric approach does not rely on specific distributional assumptions for the angular error, providing greater flexibility and broader applicability.

The structure of the paper is as follows: Section 2 introduces the proposed regression model, formulated through a generalized Möbius map that maps the real axis onto the circle, along with a discussion of the dependency of the angular error. In Section 3, we first define a novel area-based loss function for parameter estimation using the intrinsic geometry of a curved torus. This section also details the estimation method and provides two procedures for calculating coverage probability and prediction intervals. Section 4 presents extensive simulation studies. A comparative analysis with existing models is reported in Section 5. Finally, before concluding in Section 7, we analyze real-world datasets related to Bitcoin and Ethereum in Section 6.

2. REGRESSION MODEL

Regression Curve: The Möbius transformations that map the upper half plane $\text{Im}(z) > 0$ onto the open disk $|w| < 1$ and the boundary $\text{Im}(z) = 0$ of the half-plane onto the boundary $|w| = 1$ of the disk is given by

$$w = M(z; \beta_0, \beta_1) = \beta_0 \frac{z - \beta_1}{z - \bar{\beta}_1}, \quad (2.1)$$

where $\beta_0 \in \mathbb{S}_1 = \{w : |w| = 1\}$, unit circle, and $\beta_1 \in \mathbb{C}$, complex plane. Since we are interested in linear-circular regression so we must consider the map for the boundary of the upper-half

plane, $\text{Im}(z) = 0$ onto the boundary $|w| = 1$ of the disk, that is a unit circle. Hence the the regression model for response $\theta \in [0, 2\pi)$ and the predictor $x \in \mathbb{R}$ is given by

$$\theta = g(x; \beta_0, \beta_1) + \epsilon \pmod{2\pi} = [\arg(M(x; \beta_0, \beta_1))] + \epsilon \pmod{2\pi}, \quad (2.2)$$

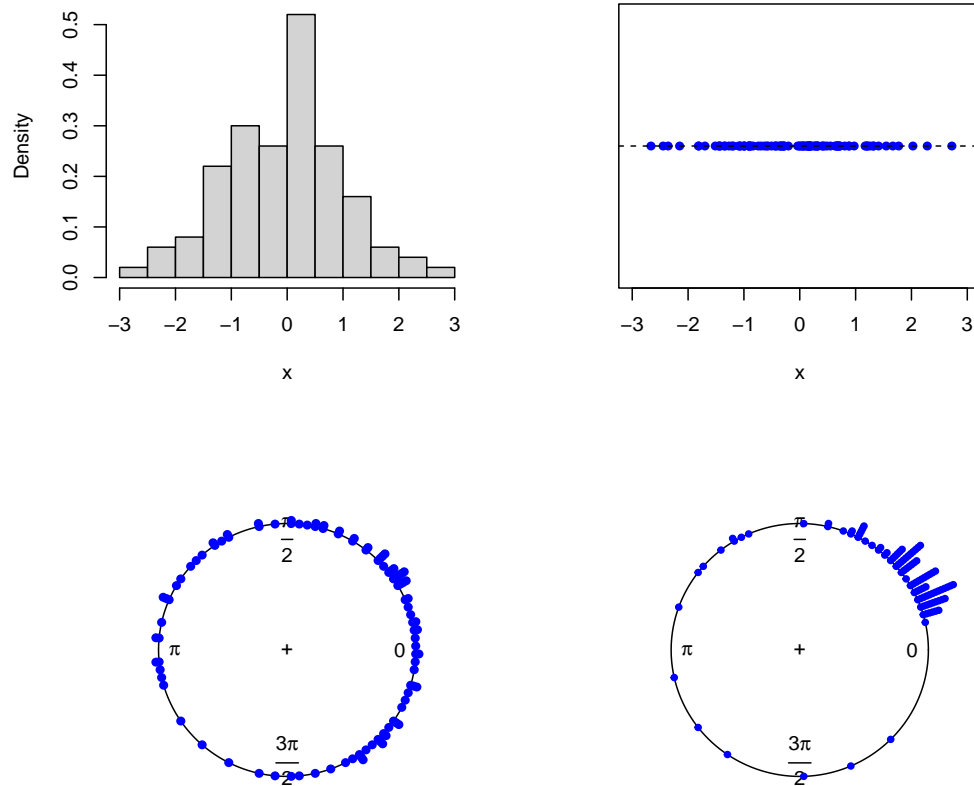


FIGURE 1. Top-left: Histogram of the predictor sampled from a standard normal distribution. Top-right: Plot of the predictor values on the real axis. Bottom-right: Plot of the response transformed through the Möbius map on unit circle. Bottom-left: Plot of the response after adding angular error drawn from a von Mises distribution.

where $g(z; \beta_0, \beta_1)$ is the link function with $\beta_0 \in \mathbb{S}_1 = \{w : |w| = 1\}$, unit circle, $\beta_1 \in \mathbb{C}$, complex plane and ϵ is a random angular error with zero mean and fixed variance. If we put the estimated value of β_0, β_1 , we would get the regression curve. Here β_0 works as a rotation parameter and without this factor, the transformation would simply map the real line to to the unit circle without any rotational adjustment. The point β_1 in the z -plane, which lies in the upper half-plane, is mapped to the origin $w = 0$ in the w -plane. This choice of β_1 as a reference

point affects the “center” of the transformation in the z -plane, effectively defining where the origin in the w -plane corresponds to the z -plane. For more detailed information, one may see [Brown and Churchill \(2009\)](#) pp. 324, Sec. 95.

It is worth noting that the angular error distribution in the proposed model is independent of any distributional assumption. The only assumption is that it has zero mean and fixed variance. Here, we only need to estimate the parameters of the Möbius map. Hence it is a semi-parametric regression model on the cylinder.

3. LOSS FUNCTION AND POINT ESTIMATION

Loss function: In least-squares regression analysis, the mean squared error (MSE) is employed as the loss function to quantify the average squared difference between the predicted values and the actual observed values. By minimizing the MSE, we estimate the model parameters that best fit the data. This minimization ensures that the predicted values are as close as possible to the observed ones, reducing the overall error in the regression model. Now, for observed values y_i and predicted values \hat{y}_i ($i = 1, 2, \dots, n$), the MSE is defined as:

$$\text{MSE} = \frac{1}{n} \sum_{i=1}^n (y_i - \hat{y}_i)^2.$$

By setting $\mathcal{Y}_i = (y_i - \hat{y}_i)^2$, for $i = 1, 2, \dots, n$, the MSE can be rewritten as $\text{MSE} = \frac{1}{n} \sum_{i=1}^n \mathcal{Y}_i^2$, which geometrically represents the mean of random squared areas in \mathbb{R}^2 .

Let $(\theta_i, x_i) \in (\mathbb{S}_1 \times \mathbb{R})$ for $i = 1, 2, \dots, n$ represent n observed data points, where \mathbb{S}_1 denotes the unit circle and \mathbb{R} represents real-valued predictors. The predicted values for θ_i are given by

$$\hat{\theta}_i = g(x_i; \beta_0, \beta_1) \pmod{2\pi}.$$

The residuals, representing the angular difference between observed and predicted values, are defined as:

$$\psi_i = (\theta_i - \hat{\theta}_i) \pmod{2\pi},$$

then motivated by this MSE and its geometric interpretation above we use the mean of “square of an angle” (see [Biswas et al., 2024](#)) for the proposed regression model and we call it mean square angle error (MSAE). To get the estimated values of the parameters β_0 , and β_1 we minimize the MSAE. Hence, the loss function can be written as

$$\mathcal{L} = \arg \min_{\beta_0, \beta_1} \frac{1}{n} \sum_{i=1}^n A_0^C(\psi_i). \quad (3.1)$$

Estimation. Since the loss function does not have a closed-form solution, numerical optimization techniques must be employed to minimize the loss function presented in Equation-3.1 and obtain the estimated values of β_0 and β_1 . In this analysis, we utilized the “L-BFGS-B” numerical optimization method, which is well-suited for problems with bounds on parameters and efficiently handles smooth, unconstrained, or constrained optimization problems. This approach ensures precise minimization of the loss function, enabling accurate parameter estimation for the proposed model.

b. CONFIDENCE INTERVAL ESTIMATION

Let $(\theta_i, x_i) \in (\mathbb{S}_1 \times \mathbb{R})$ for $i = 1, 2, \dots, n$ be n observed data points. The regression model is given by

$$\theta_i = g(x_i; \beta_0, \beta_1) + \epsilon_i \pmod{2\pi}. \quad (3.2)$$

where $g(x_i; \beta_0, \beta_1)$ is the link function with $\beta_0 \in \mathbb{S}_1 = \{w : |w| = 1\}$, unit circle, $\beta_1 \in \mathbb{C}$, complex plane and ϵ_i is a random angular error with zero mean and fixed variance for $i = 1, \dots, n$.

Algorithm for calculating coverage probability

- (1) True mean: $\mu_{\theta_i|x_i} = \text{Exp}(\theta_i) = g(x_i; \beta_0, \beta_1)$ for $i = 1, \dots, n$.
 - (2) Let $x_j \in \mathbb{R}$ be any predictor variable. Then using (1) we can write $\mu_{\theta_j|x_j} = \text{Exp}(\theta_j) = g(x_j; \beta_0, \beta_1)$.
 - (3) Get $\hat{\beta}_0, \hat{\beta}_1$, the estimated values of the parameters β_0, β_1 , then the predicted values are $\hat{\theta}_i = g(x_i; \hat{\beta}_0, \hat{\beta}_1)$ for $i = 1, \dots, n$.
 - (4) The predicted value at x_j is $\hat{\mu}_{\theta_j|x_j} = \text{Exp}(\hat{\theta}_j) = g(x_j; \hat{\beta}_0, \hat{\beta}_1)$
 - (5) Get angular error: $e_i = (\theta_i - \hat{\theta}_i) \pmod{2\pi}$ for $i = 1, \dots, n$.
 - (6) Let B be the total number of bootstraps and $\mathbf{e} = (e_1, e_2, \dots, e_n)$.
 - (7) For $b = 1, 2, \dots, B$:
 - (a) $y_i^{(b)} = [g(x_i; \hat{\beta}_0, \hat{\beta}_1) + \text{one sample with replacement from } \mathbf{e}] \pmod{2\pi}$.
 - (b) Calculate the estimated values of $\hat{\beta}_0, \hat{\beta}_1$, and call it $\hat{\beta}_0^{(b)}, \hat{\beta}_1^{(b)}$.
 - (c) Compute the response for the predictor x_j from (2) as $\hat{\theta}_j^b = g(x_j; \hat{\beta}_0^{(b)}, \hat{\beta}_1^{(b)})$
 - (8) Collect the responses for x_j from (2) as $(\hat{\theta}_j^1, \hat{\theta}_j^2, \dots, \hat{\theta}_j^B)$.
 - (9) Calculate the 95% CI from the sample in (8).
 - (10) Check whether $\mu_{\theta_j|x_j}$ from (2) and $\hat{\mu}_{\theta_j|x_j}$ and (4) fall inside the interval or not.
-

The above algorithm is performed several times to calculate the coverage probability. We consider the mean number of times those fall inside the interval. Hence we get the coverage probability.

Algorithm for calculating prediction interval

- (1) $\epsilon = (\epsilon_1, \epsilon_2, \dots, \epsilon_n)$ is from Equation-3.2.
- (2) Let $x_j \in \mathbb{R}$ be any predictor variable. Then using Equation-3.2 we write $\theta_j = g(x_j; \beta_0, \beta_1)$ one sample with replacement from $\epsilon]$ mod 2π .
- (3) Get $\hat{\beta}_0, \hat{\beta}_1$, the estimated values of the parameters β_0, β_1 , then the predicted values are $\hat{\theta}_i = g(x_i; \hat{\beta}_0, \hat{\beta}_1)$ for $i = 1, \dots, n$.
- (4) The predicted value at x_j is $\hat{\theta}_j = g(x_j; \hat{\beta}_0, \hat{\beta}_1)$
- (5) Get angular error: $e_i = (\theta_i - \hat{\theta}_i) \pmod{2\pi}$ for $i = 1, \dots, n$.
- (6) Let B be the total number of bootstraps and $\mathbf{e} = (e_1, e_2, \dots, e_n)$.
- (7) For $b = 1, 2, \dots, B$:
 - (a) $y_i^{(b)} = [g(x_i; \hat{\beta}_0, \hat{\beta}_1) + \text{one sample with replacement from } \mathbf{e}] \pmod{2\pi}$.

- (b) Calculate the estimated values of $\hat{\beta}_0, \hat{\beta}_1$, and call it $\hat{\beta}_0^{(b)}, \hat{\beta}_1^{(b)}$.
- (c) Compute the response for the predictor x_j from (2) as $\hat{\theta}_j^b = g(x_j; \hat{\beta}_0^{(b)}, \hat{\beta}_1^{(b)}) + \text{one sample with replacement from } \mathbf{e} \pmod{2\pi}$.
- (8) Collect the responses for x_j from (2) as $(\hat{\theta}_j^1, \hat{\theta}_j^2, \dots, \hat{\theta}_j^B)$.
- (9) Calculate the 95% CI from the sample in (8).
- (10) Check whether θ_j from (2) and $\hat{\theta}_j$ and (4) fall inside the interval or not.

The above algorithm is performed several times to calculate the prediction interval. We consider the mean number of times those fall inside the interval. Hence we get the prediction interval.

Note: To calculate this CI for both the algorithms, we have used *quantile.circular* function in the package *circular* by Lund et al. (2017) which is a widely used library in R programming language for circular data analysis. The pictorial representation of the same is given in Figure-2.

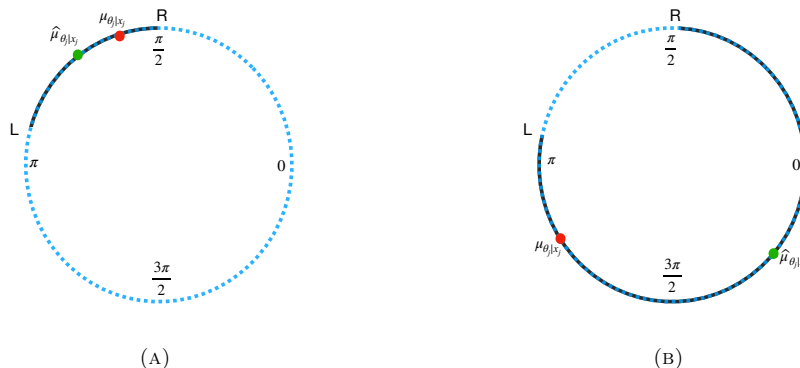


FIGURE 2. The black arc on the circle represents the CI which englobes the true and the predicted conditional means. The possible depictions of the confidence intervals on the circle can be seen in (A) and (B).

4. SIMULATION

In this section, we conduct a detailed simulation study to evaluate the performance of the proposed linear-circular regression model. The study examines the model under varying parameter settings across three sample sizes (n) to assess its robustness and effectiveness. Specifically, we consider $n = 50$ to explore small-sample behavior, $n = 150$ for moderate sample size effects, and $n = 500$ to study large-sample performance.

To demonstrate that the angular error in the proposed regression model is not dependent on the choice of distribution, we incorporate two distinct angular error distributions: the von Mises distribution and the wrapped Cauchy distribution. For both distributions, the mean direction is set to $\mu = 0$ (in radians), and simulations are performed under varying concentration parameters. This comprehensive setup allows us to investigate the behavior of the model under different distributional assumptions and sample size scenarios.

Since there exists a connection between the Normal and Cauchy distributions with the von Mises and wrapped Cauchy distributions, respectively, we generated the predictor x from the standard Normal distribution for simulations involving von Mises angular errors and from the standard Cauchy distribution for simulations involving wrapped Cauchy angular errors. However, it is important to note that the choice of distributions for both the predictor and the angular error is flexible, and other distributions can also be used depending on the application. For further details on these circular distributions and their properties, refer to [Mardia et al. \(2000\)](#).

The simulation results for the angular error models are summarized across different scenarios. When the angular error is drawn from a von Mises distribution, are summarized in Table-1 for parameter values $b_0 = 0$, $b_1 = 1.5$, and $b_2 = 0.5$, and in Table-2 for $b_0 = \frac{\pi}{6}$, $b_1 = -0.7$, and $b_2 = 2.4$. Similarly, Table-3 and Table-4 present the simulation results when the angular error is from a wrapped Cauchy distribution. Additional simulations were performed for specific conditions. Under the von Mises distribution with $b_0 = 0$, $b_1 = -1.1$, $b_2 = -1.8$, a sample size of $n = 500$, $\kappa = 5$, and zero mean direction, the parameter estimates were $\hat{b}_0 = -0.0001$ (0.0301), $\hat{b}_1 = -1.0997$ (0.0008), and $\hat{b}_2 = -1.7996$ (0.0008). For the wrapped Cauchy distribution with $b_0 = \frac{2\pi}{3}$ (≈ 2.0944), $b_1 = -0.6$, $b_2 = -0.8$, a sample size of $n = 500$, $\rho = 0.5$, and zero mean direction, the parameter estimates were $\hat{b}_0 = 2.0938$ (0.0671), $\hat{b}_1 = -0.5993$ (0.0009), and $\hat{b}_2 = -0.8001$ (0.0009). In these simulations, the parameter β_0 is represented as $\exp(ib_0)$, while β_1 is expressed as $b_1 + ib_2$. For the parameter estimates, the mean values are computed over 10,000 simulations, with the standard errors reported in parentheses for b_1 and b_2 . For b_0 , the circular mean of the estimates is presented, along with the circular variance shown in parentheses. This comprehensive representation highlights the behavior of the proposed model under various sample sizes and angular error distributions.

Figure-3(A) displays the plot of the true simulated data. The x-axis represents predictors, x , drawn from a standard normal distribution, while the y-axis represents the observed angles. These angles are derived as arguments of the transformed x through a Möbius map with parameters $b_0 = 0$, $b_1 = 1.5$, and $b_2 = 0.5$, combined with random angular errors sampled from a von Mises distribution with a zero mean direction and a concentration parameter $\kappa = 1$. Figure-3(B) shows the scatter plot of true data versus predicted data. Figure-3(C) illustrates the residual plot, showing the angular errors from the proposed linear-circular regression model applied to this simulated dataset. The residuals exhibit no discernible trend or systematic pattern, indicating that the model effectively captures the relationship between the circular and linear components. Most residuals are concentrated near zero, consistent with the assumption of minimal angular error in a well-fitted model. Additionally, the residual spread is symmetric about the zero line. Similar to how residuals in linear regression follow a normal distribution under well-met assumptions, the residuals in this model follow a von Mises (or circular normal, see [Jammalamadaka and Sengupta \(2001\)](#)) distribution. This was confirmed using Watson's test, where the test statistic (0.0259) was less than the critical value (0.079) at the 5% significance level, leading to a failure to reject the null hypothesis. Finally, Figure-3(D) compares the exact regression curve (red line) with the fitted regression curve (blue line) over the simulated dataset, highlighting the accuracy of the model.

5. COMPARISON WITH SOME EXISTING MODELS

The proposed regression model shares some similarities with the models of [Fisher and Lee \(1992\)](#) and [Kim and SenGupta \(2015\)](#). [Fisher and Lee \(1992\)](#) introduced a regression model

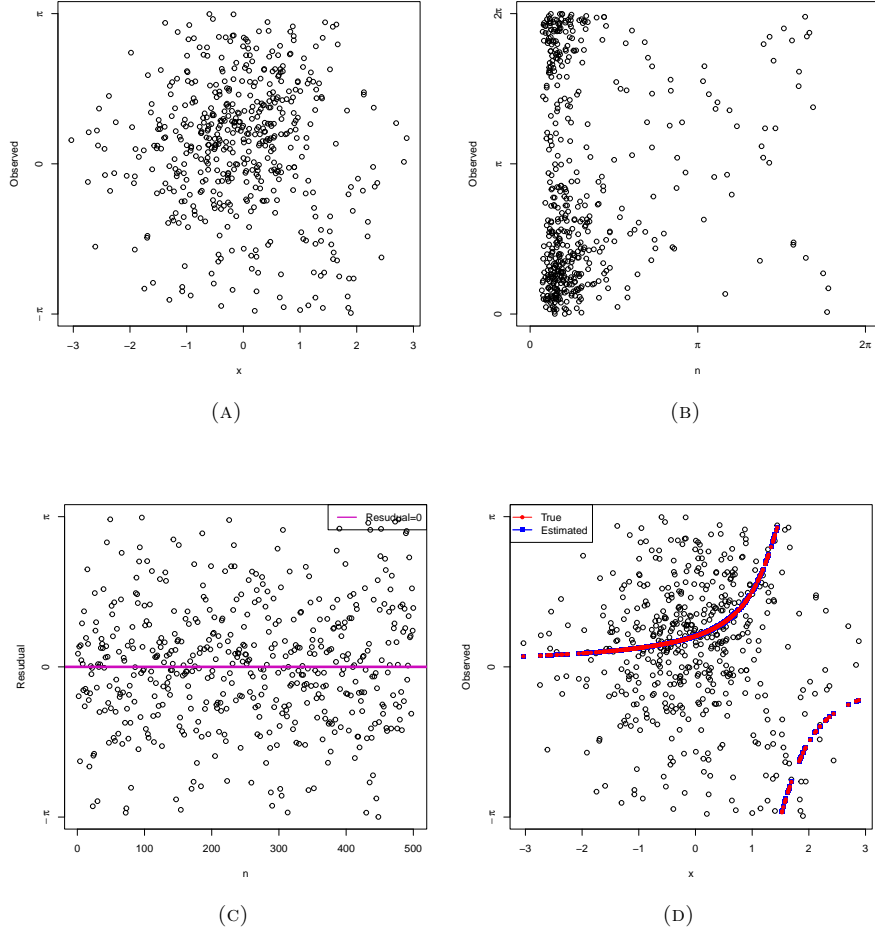


FIGURE 3. (A) Scatter plot of the true simulated data, including angular error. (B) Scatter plot comparing the true data with the predicted data. (C) Plot of the residuals (restricted to the range $[-\pi, \pi]$ for enhanced visual clarity) with a reference line at Residual = 0. (D) Plot of the exact regression curve (red line) and the fitted regression curve (blue line) overlaid on the simulated dataset.

where the link function is expressed as a form of the tangent function, while [Kim and SenGupta \(2015\)](#) employed a specific stereographic projection as a link function. Both of these models rely on the von Mises distribution for the angular error. However, our model differs from theirs in several key aspects. First, it uses a general Möbius transformation that maps the real line to the unit circle. Second, the angular error in our model is distribution-free, making it a semi-parametric regression model. Finally, we have developed a distinct cost function by applying

Sample size	Concentration parameter	Parameters		
		$b_0 = 0$	$b_1 = 1.5$	$b_2 = 0.5$
$n = 50$	$\kappa = 0.5$	0.04382 (0.3530)	1.2674 (0.0055)	0.4333 (0.0058)
	$\kappa = 1$	0.0058 (0.1346)	1.3740 (0.0040)	0.4914 (0.0042)
	$\kappa = 10$	0.0058 (0.0524)	1.4880 (0.0009)	0.4900 (0.0008)
$n = 100$	$\kappa = 0.5$	0.0015 (0.2800)	1.3945 (0.0063)	0.4592 (0.0067)
	$\kappa = 1$	0.0117 (0.1346)	1.4717 (0.0052)	0.4758 (0.0011)
	$\kappa = 10$	-0.0002 (0.0148)	1.5001 (0.0004)	0.50003 (0.0004)
$n = 500$	$\kappa = 0.5$	0.0096 (0.1300)	1.4328 (0.0031)	0.4717 (0.0027)
	$\kappa = 1$	-0.0002 (0.0692)	1.4976 (0.0011)	0.4999 (0.0011)
	$\kappa = 10$	-0.0001 (0.0307)	1.499672 (0.0002)	0.4999 (0.0002)

TABLE 1. The parameter estimates of $(b_0, b_1, b_2) = (0, 1.5, 0.5)$, with standard errors indicated in parentheses. These estimates were obtained when the predictors, sampled with varying sizes, followed a standard normal distribution, while the angular errors were drawn from a von Mises distribution with a zero mean direction and varying concentration parameters.

Sample size	Concentration parameter	Parameters		
		$b_0 = \pi/6 = 0.52359$	$b_1 = -0.7$	$b_2 = 2.4$
$n = 50$	$\kappa = 0.5$	0.6189 (0.5837)	-0.5468 (0.0198)	2.2522 (0.0166)
	$\kappa = 1$	0.5616 (0.3770)	-0.6344 (0.0097)	2.3540 (0.0093)
	$\kappa = 10$	0.5242 (0.0762)	-0.6982 (0.0016)	2.4016 (0.0019)
$n = 100$	$\kappa = 0.5$	0.5567 (0.5427)	-0.5587 (0.0170)	2.3522 (0.0155)
	$\kappa = 1$	0.5260 (0.2702)	-0.6939 (0.0068)	2.3916 (0.0062)
	$\kappa = 10$	0.5242 (0.0762)	-0.6982 (0.0016)	2.4016 (0.0019)
$n = 500$	$\kappa = 0.5$	0.5445 (0.2093)	-0.6691 (0.0007)	2.4020 (0.0007)
	$\kappa = 1$	0.5315 (0.1276)	-0.6906 (0.0004)	2.4009 (0.0003)
	$\kappa = 10$	0.5237 (0.02325)	-0.6998 (0.0007)	2.4002 (0.0007)

TABLE 2. The parameter estimates of $(b_0, b_1, b_2) = (\pi/6, -0.7, 2.4)$, with standard errors indicated in parentheses. These estimates were derived when the predictors, sampled with varying sizes, followed a standard normal distribution, and the angular errors were drawn from a von Mises distribution with a zero mean direction and varying concentration parameters.

tools from differential geometry to estimate the model parameters (constants from the Möbius map).

6. DATA ANALYSIS

Data examples: We are particularly interested in data associated with two popular cryptocurrencies: one is Bitcoin, and another is Ethereum.

- **Bitcoin:** Bitcoin, launched in 2009 by the pseudonymous Satoshi Nakamoto, operates on a decentralized peer-to-peer network using blockchain technology to enable secure, transparent transactions without intermediaries. With a capped supply of 21 million,

Sample size	Concentration parameter	Parameters		
		$b_0 = 0$	$b_1 = 1.5$	$b_2 = 0.5$
$n = 50$	$\rho = 0.3$	0.0743 (0.3978)	1.3164 (0.0045)	0.4066 (0.0044)
	$\rho = 0.6$	0.0033 (0.1816)	1.4552(0.0021)	0.4938 (0.0021)
	$\rho = 0.8$	0.0048 (0.0914)	1.4732 (0.0017)	0.4913 (0.0018)
$n = 100$	$\rho = 0.3$	-0.0114 (0.2351)	1.3835 (0.0052)	0.4578 (0.0020)
	$\rho = 0.6$	0.0182 (0.1210)	1.4696(0.0029)	0.4679 (0.0046)
	$\rho = 0.8$	-0.0015 (0.0472)	1.4990 (0.0007)	0.5008 (0.0008)
$n = 500$	$\rho = 0.3$	0.0080 (0.1007)	1.4809 (0.0022)	0.4919 (0.0020)
	$\rho = 0.6$	0.0001 (0.0431)	1.5001 (0.0006)	0.5001 (0.0007)
	$\rho = 0.8$	-0.0002 (0.0231)	1.4999 (0.0003)	0.5000 (0.0003)

TABLE 3. The parameter estimates of $(b_0, b_1, b_2) = (0, 1.7, 0.5)$, with standard errors indicated in parentheses. These estimates were obtained when the predictors, sampled with varying sizes, followed a standard Cauchy distribution, and the angular errors were drawn from a wrapped Cauchy distribution with a zero mean direction and varying concentration parameters.

Sample size	Concentration parameter	Parameters		
		$b_0 = \pi/6 = 0.52359$	$b_1 = -0.7$	$b_2 = 2.4$
$n = 50$	$\rho = 0.3$	0.5806 (0.5091)	-0.5718 (0.0016)	2.1248 (0.2372)
	$\rho = 0.6$	0.5347 (0.1945)	-0.6711 (0.0063)	2.4250 (0.0076)
	$\rho = 0.8$	0.5248 (0.1837)	-0.6886 (0.0047)	2.3940 (0.0036)
$n = 100$	$\rho = 0.3$	0.5690 (0.3510)	-0.6338 (0.0125)	2.3527 (0.0020)
	$\rho = 0.6$	0.5266 (0.1439)	-0.6894 (0.0036)	2.3955 (0.0038)
	$\rho = 0.8$	0.5263 (0.0863)	-0.6941 (0.0019)	2.4025 (0.0022)
$n = 500$	$\rho = 0.3$	0.5334 (0.1877)	-0.6826 (0.0060)	2.4053 (0.0062)
	$\rho = 0.6$	0.5256 (0.0760)	-0.6991 (0.0024)	2.4008 (0.0024)
	$\rho = 0.8$	0.5244 (0.0458)	-0.6992 (0.0001)	2.3988 (0.0009)

TABLE 4. The parameter estimates of $(b_0, b_1, b_2) = (\pi/6, -0.7, 2.4)$, with standard errors indicated in parentheses. These estimates were obtained when the predictors, sampled with varying sizes, followed a standard Cauchy distribution, and the angular errors were drawn from a wrapped Cauchy distribution with a zero mean direction and varying concentration parameters.

Bitcoin is considered a deflationary asset and is often likened to digital gold. Its decentralized nature and scarcity make it a tool for transactions and wealth preservation, attracting global investors. The blockchain ensures transaction integrity, and the Proof of Work consensus mechanism secures the network. Bitcoin’s success has spurred the development of numerous other digital currencies, establishing it as a cornerstone in digital finance.

- **Ethereum:** Introduced by Vitalik Buterin in 2015, Ethereum expanded blockchain technology beyond basic transactions, enabling the creation of smart contracts and decentralized applications (dApps). While Bitcoin primarily serves as a digital currency

and store of value, Ethereum was designed for more versatile applications. Smart contracts on Ethereum automatically execute coded agreements without intermediaries, fostering trustless transactions. Ethereum’s native currency, Ether (ETH), powers these processes, incentivizing network participation. The Ethereum Virtual Machine (EVM) allows developers to build complex dApps, spurring innovation across banking, gaming, and supply chain sectors. Ongoing upgrades, including Ethereum 2.0 and a shift to Proof of Stake, aim to enhance scalability, security, and sustainability, solidifying Ethereum’s role as a cornerstone of blockchain technology.

Data Processing: We collected per-minute historical datasets for Bitcoin and Ethereum, capturing high-frequency data to facilitate detailed analysis. Each dataset has columns for the Unix timestamp, date, symbol, opening price, highest price, lowest price, closing price, volume (in crypto), and volume (in the currency used as a base). These datasets provide a granular view of the price movements and associated timestamps, enabling precise modeling and exploration of trends, correlations, and angular relationships in financial time series data.

The date column denotes the timestamp in Coordinated Universal Time (UTC), the high column signifies the maximum price observed during the specified time, and the low column indicates the minimum price observed during the specified period.

We focus on the data associated with the highest price. Since the data was recorded at per-minute intervals, each column contains 60 data points per hour. To reduce this dataset to a single observation per hour, we select the highest value recorded within each hour. This reduction results in 24 observations per day. From these 24 hourly maximum values, we then identify the highest value across the day to determine a single observation representing the daily maximum. To compute the angular value (in radians) corresponding to the timestamp of the daily maximum, we apply the following formula:

$$\theta = \frac{\arg \max_{1 \leq j \leq 24} \left(\max_{1 \leq i \leq 60} v_i \right)_j}{24 \times 60} \in [0, 2\pi),$$

where v_i is the *highest price* of each minute. If we replace *max* by *min* in the above formula we will get the angular data corresponding to the *lowest price*.

ANALYSIS OF THE DATA

In this section, we apply our proposed semi-parametric method to two popular cryptocurrencies: Bitcoin and Ethereum. For the proposed linear-circular regression technique, we collected a Bitcoin per-minute historical dataset from Kaggle (source: <https://www.kaggle.com/datasets/prasoonkottarathil/btcinUSD?select=BTC-2017min.csv>). This dataset includes all one-minute historical data from January 1, 2017, to December 31, 2017, resulting in 365 daily observations after processing. However, this data is considered to be from January 1, 2017, to July 31, 2017, for the proposed regression model. Similarly, we collected a per-minute historical dataset for Ethereum from Kaggle (source: https://www.kaggle.com/datasets/prasoonkottarathil/ethereum-historical-dataset?select=ETH_1min.csv) which covers the period from May 9, 2016, to April 16, 2020, yielding 1409 daily observations after processing. Here, we have considered the data from January 1, 2018, to July 31, 2018, for the proposed regression model.

In modeling the timestamp of extreme cryptocurrency values (a circular variable), the opening, closing, high, and low prices can be used as linear predictors, but their effective application

requires addressing inherent complexities. Individually, these prices do not consistently correspond to specific times, as extreme values are influenced by factors such as sudden market news, liquidity shifts, and global trading activity. However, functions of these prices can encapsulate aspects like volatility, average trading levels, and directional trends that may correlate with temporal patterns. Employing such functional transformations makes it possible to reveal underlying relationships between price dynamics and the timing of extreme events, providing valuable insights into trading behavior and market structures. Specifically, we used the function

$$x = \frac{\text{lowest price}}{\text{highest price}} \times \frac{1}{(\text{closing price} - \text{opening price})}$$

as a linear predictor, with the angular representation θ of the timestamp of the high price serving as the circular response variable.

For this data analysis, we utilized the ‘‘L-BFGS-B’’ numerical optimization method. The optimization process was performed 1,000 times, each with different initial values for the parameters. Specifically, b_0 was initialized from a Uniform distribution $[0, 2\pi]$, b_1 from a Uniform distribution $[-10, 10]$, and b_2 from a Uniform distribution $[0, 10]$. The results presented in Table-5 show the estimated parameters that achieved the minimum standard error and a reasonably good QQ-plot that effectively captures the relationship in the data across these 1,000 iterations.

For the Bitcoin, Figure-5(A), and (B) show the true data and the predicted data, respectively. The residual plot in Figure-5 (C) illustrates angular errors resulting from the proposed linear-circular regression model, with the x-axis representing the index of observations (n) and the y-axis showing residual values confined to the angular range $[-\pi, \pi]$. The residuals exhibit no visible trend or systematic pattern, suggesting the model captures the relationship between circular and linear components effectively. Most residuals cluster around zero, aligning with the assumption of minimal angular error under a well-fitted model. Additionally, the spread of residuals appears symmetric about the zero line. Analogous to residuals in linear regression that follow a normal distribution under well-met assumptions, the residuals in this model follow a von Mises distribution also known as the circular normal distribution. This is confirmed through Watson’s test, where the test statistic (0.0611) was less than the critical value (0.079) at the 5% significance level, leading to a failure to reject the null hypothesis. Overall, the plot and statistical test results confirm the adequacy of the model, with the residuals being randomly distributed, centered around zero, and adhering to the theoretical assumptions for circular data. In the QQ-plot shown in Figure-5(D), the horizontal axis represents the quantiles of the observed data, while the vertical axis represents the quantiles of the predicted values. The alignment of points along a line with a 45° slope indicates that the proposed linear-circular regression model effectively captures the relationship in the data. Similarly, in the case of Ethereum, Figure-6(A), (B), (C), and (D) represent the true data, the predicted data, the residual plot, and the QQ-plot, respectively. Here, the residuals also follow a von Mises distribution, as confirmed by Watson’s test. The test statistic of 0.0581 was below the critical value of 0.079 at the 5% significance level, leading to a failure to reject the null hypothesis.

7. CONCLUSION

In this study, we have introduced a novel area-based regression model designed to address scenarios where responses are angular variables and predictors are linear. By leveraging the generalized Möbius transformation to define the regression curve, we seamlessly map the real axis to the circle, capturing the intrinsic relationship between linear and angular components.

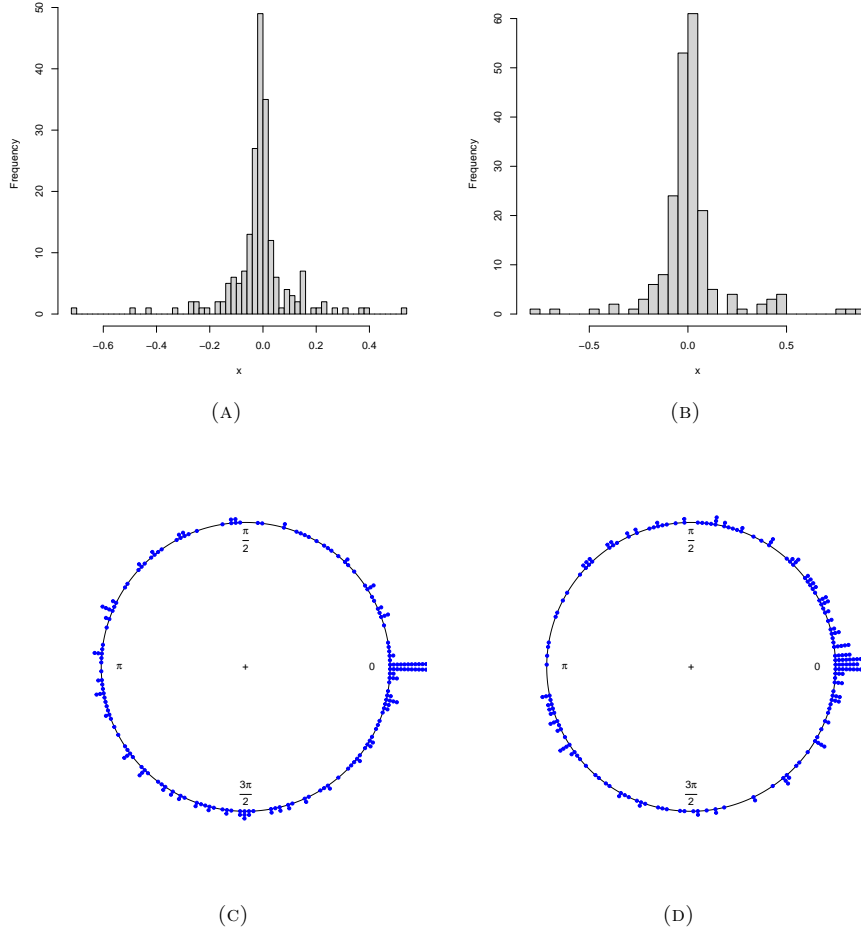


FIGURE 4. (A) and (B): Histograms of the predictor for Bitcoin and Ethereum, respectively. (C) and (D): Circular plots of the response angles corresponding to the timestamps of the high prices for Bitcoin and Ethereum, respectively.

A key feature of our model is the area-based loss function, rooted in the geometry of a curved torus, which allows for efficient parameter estimation. Importantly, the semi-parametric nature of the model eliminates the need for specific distributional assumptions about the angular error, broadening its applicability. Through extensive simulation studies with von Mises and wrapped Cauchy distributions, we have demonstrated the robustness and flexibility of the proposed framework. The practical utility of the model was further validated through real-world data analysis involving two major cryptocurrencies, Bitcoin and Ethereum, showcasing its capability to extract meaningful insights from complex datasets. These results highlight the potential of the proposed regression model as a powerful tool for analyzing circular-linear relationships in various applied contexts.

Digital Currency	Estimated value of b_0 with standard error, \hat{b}_0 (s.e) in radian	Estimated value of b_1 with standard error, \hat{b}_1 (s.e)	Estimated value of b_2 with standard error, \hat{b}_2 (s.e)	Correlation
Bitcoin	2.7836 (4.8660)	-0.0068(0.1511)	0.0362 (0.3097)	0.7430
Ethereum	2.2596 (4.5086)	-0.0310 (0.3548)	0.0702 (0.5870)	0.7597

TABLE 5. Estimated parameter values (with standard errors) and correlations between the predictor and response for Bitcoin and Ethereum data.

8. ACKNOWLEDGEMENT

The authors are thankful to Mr. Shabhunath Sen, a doctoral candidate at the Department of Mathematics, Indian Institute of Technology Kharagpur, India, for helpful discussion.

9. FUNDING

S. Biswas expresses gratitude for the financial support received through a Junior/Senior Research Fellowship from the Ministry of Human Resource Development (MHRD) and IIT Kharagpur, India. B. Banerjee acknowledges the funding provided by the Science and Engineering Research Board (SERB), Department of Science and Technology, Government of India, under the MATRICS grant (File No. MTR/2021/000397).

10. AUTHOR CONTRIBUTIONS

SB and BB wrote the main manuscript text. SB has done data analysis and prepared all figures and tables. All authors reviewed the manuscript.

REFERENCES

- Biswas, S., Banerjee, B., and Laha, A. K. (2024). Changepoint problem with angular data using a measure of variation based on the intrinsic geometry of torus. *arXiv preprint arXiv:2403.00508*.
- Brown, J. W. and Churchill, R. V. (2009). *Complex variables and applications*. McGraw-Hill.
- Downs, T. (2003). Spherical regression. *Biometrika*, 90(3):655–668.
- Downs, T. D. and Mardia, K. (2002). Circular regression. *Biometrika*, 89(3):683–698.
- Fisher, N. I. and Lee, A. J. (1992). Regression models for an angular response. *Biometrics*, pages 665–677.
- Jammalamadaka, S. R. and Sengupta, A. (2001). *Topics in circular statistics*, volume 5. world scientific.
- Jha, J. and Biswas, A. (2018). Circular-circular regression model with a spike at zero. *Statistics in Medicine*, 37(1):71–81.
- Kato, S., Shimizu, K., and Shieh, G. S. (2008). A circular–circular regression model. *Statistica Sinica*, pages 633–645.
- Kim, S. and SenGupta, A. (2015). Inverse circular–linear/linear–circular regression. *Communications in Statistics-Theory and Methods*, 44(22):4772–4782.

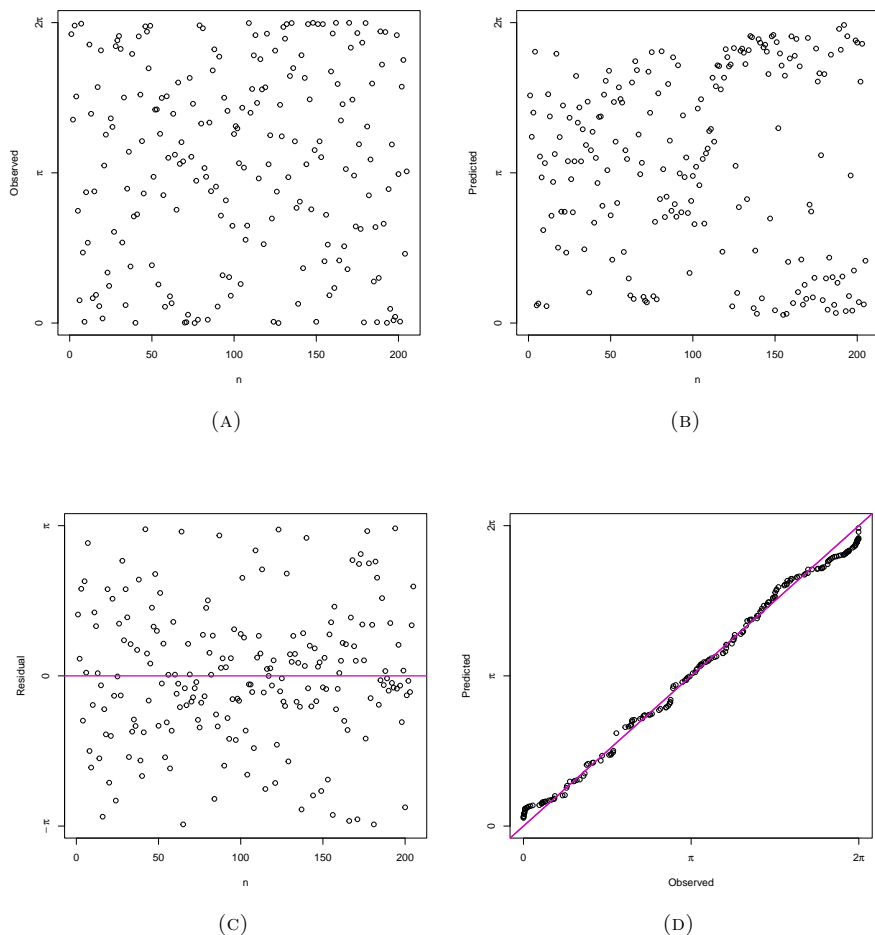


FIGURE 5. For Bitcoin: (A) Scatter plot of the angles corresponding to the timestamps of the high prices. (B) Scatter plot of the predicted angles for the timestamps of the high prices. (C) Plot of the residuals (restricted to the range $[-\pi, \pi]$ for improved visual clarity) with a reference line at Residual = 0.. (D) QQ plot (on a radian scale) compares the observed angles with the predicted angles from the proposed model.

Lund, U., Agostinelli, C., and Agostinelli, M. C. (2017). Package ‘circular’. *Repository CRAN*, 775(5).

Mardia, K. V., Jupp, P. E., and Mardia, K. (2000). *Directional statistics*, volume 2. Wiley Online Library.

McCullagh, P. (1996). Möbius transformation and cauchy parameter estimation. *The Annals of Statistics*, 24(2):787–808.

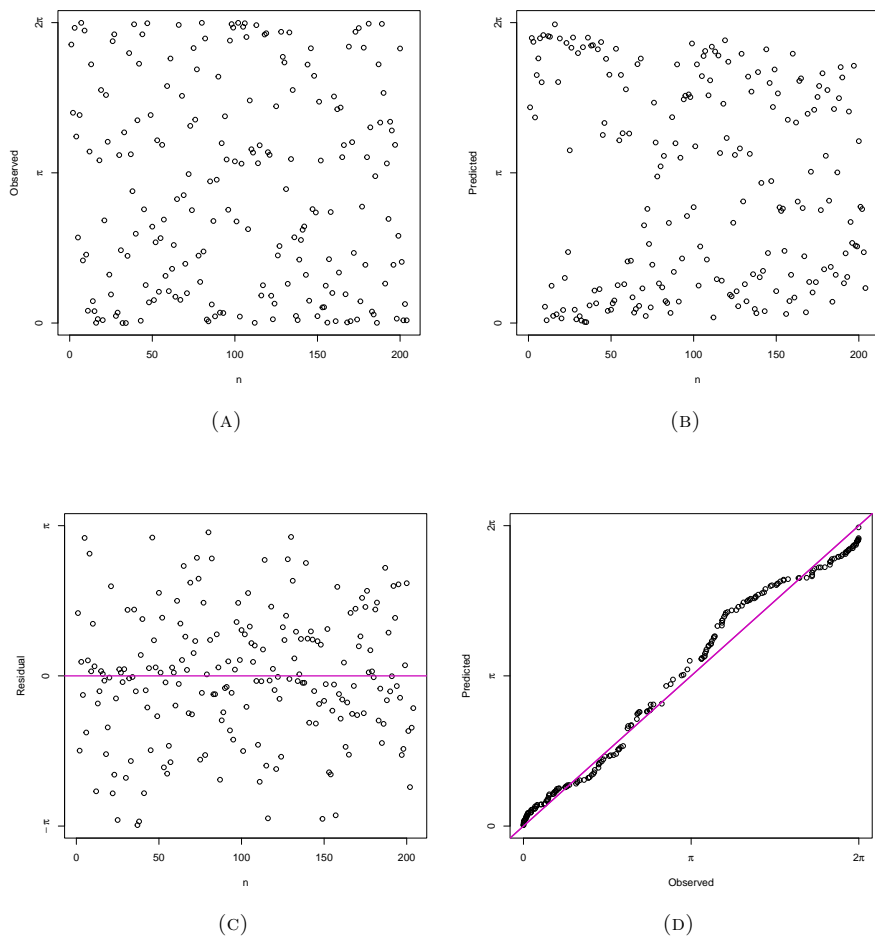


FIGURE 6. For Ethereum: (A) Scatter plot of the angles corresponding to the timestamps of the high prices. (B) Scatter plot of the predicted angles for the timestamps of the high prices. (C) Plot of the residuals (restricted to the range $[-\pi, \pi]$ for improved visual clarity) with a reference line at Residual = 0. (D) QQ plot (on a radian scale) compares the observed angles with the predicted angles from the proposed model.